IEEE Access
Multidisciplinary | Rapid Review | Open Access Journal

Received April 26, 2021, accepted May 12, 2021, date of publication May 17, 2021, date of current version May 27, 2021.

Digital Object Identifier 10.1109/ACCESS.2021.3081443

Joint Estimation of Driving State and Road Adhesion Coefficient for Distributed Drive Electric Vehicle

YANAN WU, GANG LI, AND DONGSHENG FAN
Automobile and Traffic Engineering College, Liaoning University of Technology, Jinzhou 121001, China
Corresponding author: Gang Li (qcxyligang@lnut.edu.cn)

This work was supported by the National Natural Science Foundation of China under Grant 51675257.

ABSTRACT Obtaining accurate vehicle driving state and road adhesion coefficient information is of great significance to many aspects of the vehicle. This paper takes distributed drive electric vehicles as the research object and designs a joint estimation method of vehicle driving state and road adhesion coefficient based on the theory of federated-cubature Kalman filter. The corresponding nonlinear three-degree-of-freedom vehicle dynamics model is established and the state space equation is obtained. Multi-source fusion of low-cost sensor signals is carried out by using information fusion technology, and an algorithm estimator is built by using vehicle dynamics theory. Select typical experimental conditions and apply Simulink to build an algorithm model and co-simulate with CarSim for verification. The experimental results show that the proposed estimation method can improve the accuracy and stability of state estimation.

INDEX TERMS Distributed drive electric vehicle, driving state estimation, federal-cubature Kalman filter, information fusion, road adhesion coefficient, simulation verification.

I. INTRODUCTION

With the low-carbon and zero-emission development advocated by people in today's society, the promotion of electric vehicles to replace traditional fuel vehicles has become one of the effective means for the transformation of the automotive industry in recent years. As one of the important development directions of electric vehicles, distributed drive electric vehicles have brought significant advantages for vehicles in terms of active safety control and stability control [1], [2]. Accurate acquisition of vehicle key states and road adhesion coefficients is a prerequisite for active vehicle safety control and stability control. But for the estimation of these important parameter variables, algorithm model estimators are commonly used. The road adhesion coefficient in the algorithm model usually directly adopts a fixed value, and the influence of these parameter changes is mostly ignored in the process of estimating the driving state of the vehicle. Besides, during the driving of the car, due to the continuous changes of the working conditions, these parameter variables also change continuously, which affects the accuracy of the estimation of the driving state. Therefore, it is particularly important to consider the change of the road adhesion coefficient in the process of estimating the driving state of the vehicle.

In recent years, domestic and foreign scholars have successively proposed a variety of methods for the estimation of road adhesion coefficient. Reference [3] proposed a method of integrating a friction estimator based on a smart tire with an estimator based on a brush tire model. This method can reliably estimate the coefficient of friction under a wider range of excitations (low slip and high slip conditions). Reference [4] proposed an online estimation method of the bounded maxi-mum friction coefficient of series sensors based on sensitivity and joint unscented Kalman filter. By introducing local sensitivity analysis, robust estimation of drift without parameter estimation can be achieved under the condition of insufficient excitation. Reference [5] proposed a specific nonlinear tire model estimation method based on the unscented Kalman filter to estimate the lateral and longitudinal friction and the friction coefficient of the wheel. Reference [6] designed a vehicle driving state estimator and a road adhesion coefficient estimator based on dual CKF for distributed-drive front-wheel steering electric vehicles. By linking the two together to form a closed-loop system, an accurate estimation of the road adhesion coefficient is achieved. Reference [7] uses the advantages

The associate editor coordinating the review of this manuscript and approving it for publication was Shihong Ding.

and characteristics of distributed drive electric vehicles to establish a dual Kalman filter fusion estimation algorithm, which estimates road adhesion coefficient and vehicle speed independent of each other, and verifies the effectiveness of the algorithm through actual vehicles. Reference [8] considers that the variability of model parameters can easily lead to the problem of excessive filtering errors or even divergence, and thus introduces exponentially weighted decay memory filtering. A road adhesion coefficient estimator is designed based on UKF, which further improves the estimation accuracy. Reference [9] proposed an improved parallel strong tracking road adhesion coefficient estimation algorithm based on unscented Kalman theory. It constructs two two-dimensional observers with a single fading factor matrix, which can observe the road adhesion coefficients of four tires of electric vehicles in real-time. Reference [10] combined the Pacejka tire model and UKF theory to estimate the tire longitudinal force and wheel slip rate, and the slope of the slip rate curve corresponding to different road adhesion coefficients can be obtained. Then through the relationship between the different road adhesion coefficient and the slope of the slip rate curve to obtain the road adhesion coefficient. Reference [11] uses the extended Kalman filter to estimate the lateral speed of the vehicle. The wheel speed sensor datas are estimated by a specific algorithm to obtain the longitudinal speed of the car, and then the sideslip angle information of the center of mass is obtained, and then the state information is combined with the extended Kalman filter to estimate the road adhesion coefficient. Reference [12] is based on RLS and introduces a forgetting factor to reduce the influence of irrelevant information, and builds a road adhesion coefficient observer, which can realize real-time estimation of road adhesion coefficient under various conditions. Reference [13] uses the seven-degree-of-freedom vehicle model and the extended Kalman filter to estimate the longitudinal and lateral speed of the car. By calculating the tire slip angle and using the back-propagation neural network method, the road adhesion coefficient is estimated. Reference [14] used a nonlinear filter to estimate the longitudinal slip rate of the wheel by collecting sensor signals. Then use the Kalman filter to estimate the tire force, and use these parameters to estimate the friction coefficient between the tire and the road through the recursive least square method.

Aiming at the problems of low estimation accuracy and poor real-time performance of ordinary algorithms, this paper proposes a federated-cubature Kalman filter estimation algorithm. Federal Kalman Filter (FKF) is gradually developed based on decentralized filtering. It is mostly used in military navigation fields that require high accuracy and robustness. It has only been gradually applied to the automotive field in recent years. It usually contains two layers of filter structure, one layer has several sub-filter structures, and the other layer is the main filter structure. The core idea is the principle of ''information distribution'', that is, the global state information and system noise matrix are dispersed and distributed to each sub-filter, and then the estimated information of each sub-filter is integrated through the main filter to achieve the optimal fusion estimation. The structure does not change the unique form of the sub-filter structure so that it has the characteristics of flexible design and good fault tolerance [15]. To improve the estimation accuracy of the algorithm and ensure the real-time performance of the algorithm, this paper selects the fusion reset structure and uses two sub-filters and one main filter to design. For the time update and measurement update in each sub-filter, the cubature Kalman filter algorithm is used. This combined method makes full use of their respective advantages and can make the process noise adaptively change during the estimation process, that is, take different values at different moments, and continuously modify the process noise statistical parameters in real-time. It effectively solves the problem of divergence of estimation results [16], so that the algorithm not only has good fault tolerance and stability but also improves the estimation accuracy of the algorithm.

The rest of this paper is organized as follows. The vehicle dynamics model and tire model are presented in Section II. The joint estimation of driving state and road adhesion coefficient for distributed drive electric vehicle designed in Section III. In Section IV, we conduct software simulations and results analysis. Finally, in Section V, we summarize the conclusions and propose future work.

II. VEHICLE ESTIMATION MODEL

A. DISTRIBUTED-DRIVE ELECTRIC VEHICLE DYNAMICS MODEL

The vehicle dynamics model represents the mathematical relationship between different parameter variables during the motion of a vehicle and is the basis for designing the vehicle state and road adhesion coefficient estimation algorithms. For distributed-drive electric vehicles, the three-degree-of-freedom (3-DOF) vehicle estimation model is built based on the traditional 2-DOF model [17], considering the timeliness of the entire estimation algorithm and the three aspects of longitudinal, lateral, and yaw. The nonlinear 3-DOF vehicle model is shown in Fig. 1 and the following assumptions are made:

(1) The origin of vehicle coordinate system coincides with the mass center of the vehicle estimation model.
(2) Suppose the vehicle is composed of a rigid body and four wheels that are controlled independently of each other.
(3) Assuming that the mechanical characteristics of the tires are the same.
(4) The effect of the suspension system is ignored.

In Fig. 1, a and b are distance from the center of centroid position to the front and rear axles, t_f and t_r are the front and rear wheel tread, υ_{ij} is the wheel center speed, δ_{ij} is the four-wheel angle obtained directly through the steering motor, F_{x_ij} is the longitudinal force of the tire, F_{y_ij} is the lateral force of the tire, and α_{ij} is side-slip angle of the tire. Among them, i represents the front or rear wheel and j represents the left or right wheel.

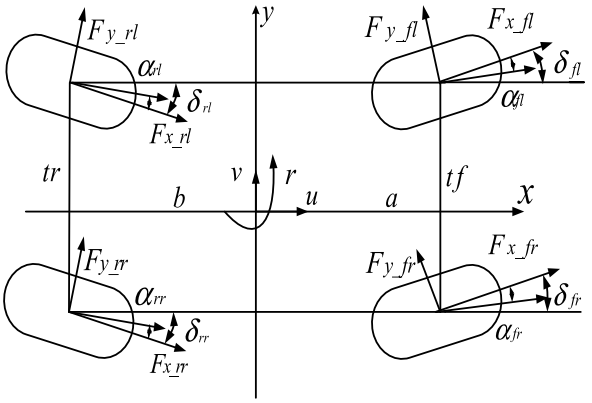

FIGURE 1. Vehicle dynamics mode.

The dynamics equations of vehicle model are as follows:

$$\dot{u} = a_x + vr \tag{1}$$

$$\dot{v} = a_y - ur \tag{2}$$

$$\dot{r} = \frac{1}{I_z}\Gamma \tag{3}$$

where u and v are the longitudinal/lateral velocity, a_x and a_y are the longitudinal/lateral acceleration, r is the yaw rate, I_z is the moment of inertia about z-axis and Γ is the yaw moment.

Based on the dynamics equations, a_x, a_y and Γ are calculated by:

$$\begin{aligned} a_x = \frac{1}{m}(&F_{x\_fl}\cos\delta_{fl} - F_{y\_fl}\sin\delta_{fl} \\ &+ F_{x\_fr}\cos\delta_{fr} - F_{y\_fr}\sin\delta_{fr} \\ &+ F_{x\_rl}\cos\delta_{rl} + F_{y\_rl}\sin\delta_{rl} \\ &+ F_{x\_rr}\cos\delta_{rr} + F_{y\_rr}\sin\delta_{rr}) \end{aligned} \tag{4}$$

$$\begin{aligned} a_y = \frac{1}{m}(&F_{x\_fl}\sin\delta_{fl} + F_{y\_fl}\cos\delta_{fl} \\ &+ F_{x\_fr}\sin\delta_{fr} + F_{y\_fr}\cos\delta_{fr} \\ &- F_{x\_rl}\cos\delta_{rl} + F_{y\_rl}\sin\delta_{rl} \\ &- F_{x\_rr}\cos\delta_{rr} - F_{y\_rr}\sin\delta_{rr}) \end{aligned} \tag{5}$$

$$\begin{aligned} \Gamma = &a(F_{x\_fl}\sin\delta_{fl} + F_{y\_fl}\cos\delta_{fl}) \\ &- \frac{t_f}{2}(F_{x\_fl}\cos\delta_{fl} - F_{y\_fl}\sin\delta_{fl}) \\ &+ a(F_{x\_fr}\sin\delta_{fr} + F_{y\_fr}\cos\delta_{fr}) \\ &+ \frac{t_f}{2}(F_{x\_fr}\cos\delta_{fr} - F_{y\_fr}\sin\delta_{fr}) \\ &+ b(F_{x\_rl}\cos\delta_{rl} - F_{y\_rl}\sin\delta_{rl}) \\ &- \frac{t_r}{2}(F_{x\_rl}\cos\delta_{rl} + F_{y\_rl}\sin\delta_{rl}) \\ &+ b(F_{x\_rr}\cos\delta_{rr} - F_{y\_rr}\sin\delta_{rr}) \\ &+ \frac{t_r}{2}(F_{x\_rr}\cos\delta_{rr} - F_{y\_rr}\sin\delta_{rr}) \end{aligned} \tag{6}$$

where the slip angle, line speed and normal reaction force of the four wheels are calculated by:

$$\begin{aligned} \alpha_{fl,fr} &= \delta_{fl,fr} - \arctan\left(\frac{v + ar}{u \pm \frac{t_f}{2}r}\right) \\ \alpha_{rl,rr} &= \delta_{rl,rr} - \arctan\left(\frac{-v + br}{u \pm \frac{t_r}{2}r}\right) \end{aligned} \tag{7}$$

$$\begin{aligned} v_{fl,fr} &= \sqrt{(u \pm \frac{t_f}{2})^2 + (v + ar)^2} \\ v_{rl,rr} &= \sqrt{(u \pm \frac{t_r}{2})^2 + (v - br)^2} \end{aligned} \tag{8}$$

$$\begin{aligned} F_{z\_fl,fr} &= (\frac{1}{2}mg \pm ma_y\frac{h}{t_f})\frac{b}{l} - \frac{1}{2}ma_x\frac{h}{l} \\ F_{z\_rl,rr} &= (\frac{1}{2}mg \pm ma_y\frac{h}{t_r})\frac{b}{l} + \frac{1}{2}ma_x\frac{h}{l} \end{aligned} \tag{9}$$

where F_{z_ij} is the normal reaction force of the ground to the wheel, m is the mass of the vehicle, l is the wheelbase and h is the height of the center of mass.

The four-wheel longitudinal force can be calculated by:

$$F_{x\_ij} = \frac{T_{ij} - J_{ij}\cdot\dot{\omega}_{ij}}{R_e} \tag{10}$$

where T_{ij} is the driving torque of the four wheels, J_{ij} represents the moment of inertia of the four wheels, ω_{ij} represents the angular acceleration of the four wheels.

B. DUGOFF TIRE MODEL

The Dugoff tire model [18] is used in the vehicles estimation model. The tire model can directly obtain the lateral force of the tire through the slip rate. The formula is as shown in (11) ∼ (14):

$$F_{y\_ij} = \mu_{\_ij}F_{z\_ij}C_y\frac{\tan(\alpha_{ij})}{1 - \lambda_{\_ij}}f(L) \tag{11}$$

where μ_{ij} is the road adhesion coefficient, C_y is the tire cornering stiffness, $\lambda_{\_ij}$ is the longitudinal slip rate.

$$f(L) = \begin{cases} L.(2 - L), & L < 1 \\ 1, & L \geq 1 \end{cases} \tag{12}$$

$$\begin{aligned} L = &\frac{1}{\sqrt[2]{C_x^2\lambda_{\_ij}^2 + C_y^2\tan^2\alpha_{ij}}}(1 - \lambda_{\_ij}) \\ &\times (1 - \varepsilon\cdot u\cdot\sqrt{C_x^2\lambda_{\_ij}^2 + C_y^2\tan^2\alpha_{ij}}) \end{aligned} \tag{13}$$

where C_x is the longitudinal stiffness of the tire and ε is the impact factor of velocity.

The corresponding slip rate equations for braking and driving were calculated by using (14).

$$\begin{aligned} \lambda_{ij} &= \frac{R_e\,\omega_{ij} - v_{ij}}{v_{ij}} = \frac{R_e\,\omega_{ij}}{v_{ij}} - 1 < 0 \quad (brake) \\ \underset{ij}{\lambda} &= \frac{R_e\,\omega_{ij} - v_{ij}}{R_e\,\omega_{ij}} = 1 - \frac{v_{ij}}{R_e\,\omega_{ij}} > 0 \quad (drive) \end{aligned} \tag{14}$$

Since the value of tire longitudinal stiffness and lateral stiffness is affected by many factors, such as its own structure, specifications and dimensions, inflation pressure, load, and various driving conditions, etc, among which the load has the greatest impact on these two parameters. Therefore, this paper only considers the impact of the load on the tire, ignoring the impact of other complex factors. Through the standard tire model parameters in the simulation software CarSim, the longitudinal and lateral stiffness values of a group of tires

TABLE 1. Value of tire longitudinal stiffness and lateral stiffness.

Load (N)	800	1200	2400	3600	4800
Longitudinal stiffness C_x (N/rad)	17660	26500	53370	84060	110230
Lateral stiffness C_y (N/rad)	23600	35400	70500	10400	25350

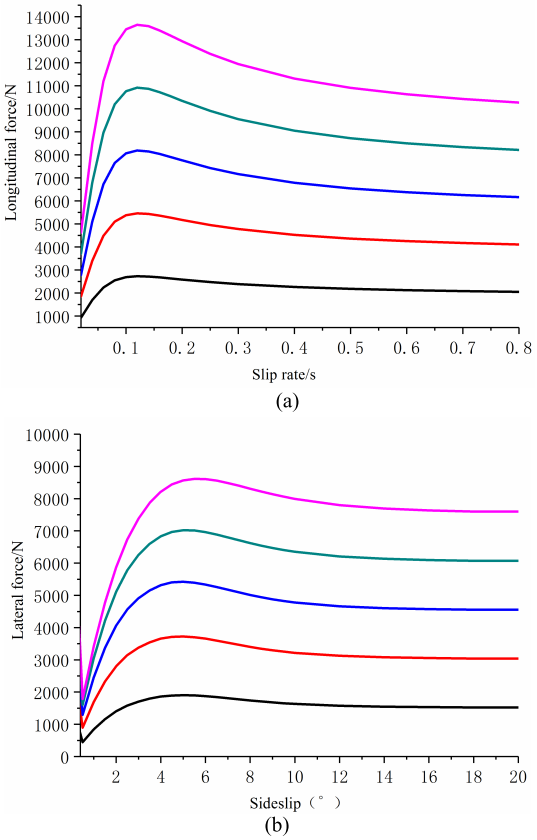

FIGURE 2. Tire characteristic diagram: (a) Tire longitudinal slip characteristic diagram; (b) Tire side deflection characteristic diagram.

under different loads are obtained by interpolation, as shown in Table 1.

Fig. 2 reflects the tire characteristics of the tire model under different loads.

III. DESIGN FOR DRIVING STATE AND ROAD ADHESION COEFFICIENT ESTIMATION ALGORITHM

A. PRINCIPLE OF ESTIMATION ALGORITHM

The principle of joint estimation of driving state and road adhesion coefficient for distributed drive electric vehicle is shown in Fig. 3. It can be seen from the figure that the vehicle-mounted sensor signals are collected through the vehicle communication network, which mainly includes the longitudinal acceleration, lateral acceleration, yaw rate,

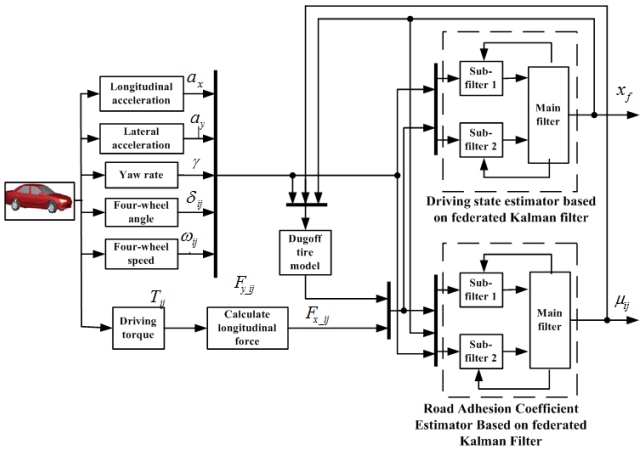

FIGURE 3. Joint estimation schematic.

four-wheel angle, four-wheel speed, and four-wheel-drive torque. These sensor signals are simultaneously transmitted to the main/sub-filters in the driving state estimator and the adhesion coefficient estimator, as well as the Dugoff tire model as the signal input of the algorithm model. The tire lateral force is calculated through the tire model, and the collected four-wheel-drive torque is directly converted into the longitudinal force of the four wheels through the tire longitudinal force calculation module. Its purpose is to reduce the error caused by the tire model itself in calculating the tire force. The tire force obtained is used as another input of each main/sub filter in the driving state estimator and the adhesion coefficient estimator. The difference with the independent driving state estimator is that the road adhesion coefficient no longer takes a fixed value, but receives the estimated value from the algorithm estimator. The main filters in the two joint estimators are initialized after receiving these signals, and the default value of the information distribution coefficient is zero. The driving state variables, adhesion coefficient variables, covariance matrix, and process noise matrix are assigned to each sub-filter accordingly, and then each sub-filter integrates the received sensor signal and the distributed signal. First, completes the time update to obtain the prior state estimation value, and then completes the measurement update according to the respective measurement values to obtain the posterior partial estimation value, and then pass the datas to the main filter for integration to complete the global optimal estimation. The optimal estimate is used as the output and at the same time, information is distributed again to each sub-filter according to a specific distribution principle, so as to complete an iteration. Iteratively over time, a closed-loop is formed in the driving state estimator and the adhesion coefficient estimator. At the same time, the estimated value of the global optimal driving state is fed back to the road adhesion coefficient estimator and the tire model. The estimated value of the global optimal road adhesion coefficient is fed back to the driving state estimator and the tire model, and its state parameters are continuously modified to form a closed loop. It completes the joint accurate

estimation of the vehicle driving state and the road adhesion coefficient.

B. JOINT ESTIMATION ALGORITHM

The specific algorithm such as formulas (15) to (54).

1) THE INFORMATION DISTRIBUTION PROCESS OF VEHICLE DRIVING STATE

First, the driving state variables, error covariance matrix, and system process noise covariance matrix are distributed to each sub-filter according to the principle of information distribution through the main filter.

$$X^{\wedge}_{si,k-1} = X_{sf,k-1} \tag{15}$$
$$P^{-1}_{si,k-1} = \beta_{si} P^{-1}_{sf,k-1} \tag{16}$$
$$Q^{-1}_{si,k-1} = \beta_{si} Q^{-1}_{sf,k-1} \tag{17}$$

where β_{si} is the distribution coefficient of driving state information, $i = 1, 2$ (i.e. two sub-filters), according to the principle of information conservation, there is $\beta_{s1} + \beta_{s2} = 1$.

2) THE INFORMATION DISTRIBUTION PROCESS OF ROAD ADHESION COEFFICIENT

Through the main filter, the parameter variables of the road adhesion coefficient, the error covariance matrix, and the system process noise covariance matrix are allocated to each sub-filter according to the principle of information distribution.

$$X^{\wedge}_{pi,k-1} = X_{pf,k-1} \tag{18}$$
$$P^{-1}_{pi,k-1} = \beta_{pi} P^{-1}_{pf,k-1} \tag{19}$$
$$Q^{-1}_{pi,k-1} = \beta_{pi} Q^{-1}_{pf,k-1} \tag{20}$$

where β_{pi} is the distribution coefficient of driving state information, $i = 1, 2$ (i.e. two sub-filters), according to the principle of information conservation, there is $\beta_{p1} + \beta_{p2} = 1$.

3) THE TIME UPDATE PROCESS OF VEHICLE DRIVING STATE

The time update is performed independently in each driving state sub-filter.

① To decompose the covariance matrix $P_{s,k-1}$ through SVD

$$P_{s,k-1} = A_{s,k-1} \Lambda_{s,k-1} A^{T}_{s,k-1} \tag{21}$$

where $A_{s,k-1}$ is the characteristic matrix corresponding to the driving state covariance matrix $P_{s,k-1}$, $\Lambda_{s,k-1} = diag[S^2_{s1,k-1}, S^2_{s2,k-1} \ldots\ldots, S^2_{sn,k-1}]$, $S^2_{si,k-1}$ is the square root of the eigenvalues corresponding to $P_{s,k-1}$.

② The cubature point of the previous moment

$$X_{sj,k-1} = A_{si,k-1} S_{si,k-1} \xi_j + X^{\wedge}_{s,k-1} \tag{22}$$

where $i = 1, 2 \ldots\ldots n$, n is the dimension of the driving state variable, ξ_j is the cubature point, and $\xi_j = \sqrt{\frac{m}{2}}\,[1]_j$, $j = 1, 2 \ldots\ldots m$, m is the number of cubature points and the size is twice the dimension of the driving state variable, $[1]_j$ represents the j-th cubature point element.

In this paper, the number of vehicle driving state variables is $n = 6$, then the cubature point set is:

$$\left\{ \begin{bmatrix} 1\\0\\0\\0\\0\\0 \end{bmatrix}, \begin{bmatrix} 0\\1\\0\\0\\0\\0 \end{bmatrix}, \begin{bmatrix} 0\\0\\1\\0\\0\\0 \end{bmatrix}, \begin{bmatrix} 0\\0\\0\\1\\0\\0 \end{bmatrix}, \begin{bmatrix} 0\\0\\0\\0\\1\\0 \end{bmatrix}, \begin{bmatrix} 0\\0\\0\\0\\0\\1 \end{bmatrix}, \begin{bmatrix} -1\\0\\0\\0\\0\\0 \end{bmatrix}, \begin{bmatrix} 0\\-1\\0\\0\\0\\0 \end{bmatrix}, \begin{bmatrix} 0\\0\\-1\\0\\0\\0 \end{bmatrix}, \begin{bmatrix} 0\\0\\0\\-1\\0\\0 \end{bmatrix}, \begin{bmatrix} 0\\0\\0\\0\\-1\\0 \end{bmatrix}, \begin{bmatrix} 0\\0\\0\\0\\0\\-1 \end{bmatrix} \right\}.$$

③ The cubature point after iteration of the system equation

$$X^{*}_{sj,k/k-1} = f\left(X_{sj,k/k-1}, U_k\right) \tag{23}$$

④ The predicted value after time update

$$X^{\wedge}_{s,k/k-1} = \sum_{j=1}^{m} \frac{1}{m} X^{*}_{sj,k/k-1} \tag{24}$$

⑤ The predicted value of the error covariance matrix

$$P_{s,k/k-1} = \sum_{j=1}^{m} \frac{1}{m} X^{*}_{sj,k/k-1} X^{*T}_{sj,k/k-1} - X^{\wedge}_{s,k/k-1} X^{\wedge T}_{s,k/k-1} + Q_s \tag{25}$$

where Q_s is the process noise covariance matrix of the driving state.

4) THE TIME UPDATE PROCESS OF ROAD ADHESION COEFFICIENT

The time update is performed independently in each road adhesion coefficient sub-filter.

① To decompose the covariance matrix $P_{p,k-1}$ based on SVD

$$P_{p,k-1} = A_{p,k-1} \Lambda_{p,k-1} A^{T}_{p,k-1} \tag{26}$$

where $A_{p,k-1}$ is the characteristic matrix corresponding to the road adhesion coefficient covariance matrix $P_{p,k-1}$, $\Lambda_{p,k-1} = diag[S^2_{p1,k-1}, S^2_{p2,k-1} \ldots\ldots, S^2_{pn,k-1}]$, $S^2_{pi,k-1}$ is the square root of the eigenvalues corresponding to $P_{p,k-1}$.

② The cubature point of the previous moment

$$X_{pj,k-1} = A_{pi,k-1} S_{pi,k-1} \xi_j + X^{\wedge}_{p,k-1} \tag{27}$$

where $i = 1, 2 \ldots\ldots n$, n is the dimension of the driving state variable, ξ_j is the cubature point, and $\xi_j = \sqrt{\frac{m}{2}}\,[1]_j$, $j = 1, 2 \ldots\ldots m$, m is the number of cubature points and the size is twice the dimension of the driving state variable, $[1]_j$ represents the j-th cubature point element.

In this paper, the number of road adhesion coefficient parameter variables is 4, and the cubature point set is:

$$\left\{\begin{bmatrix}1\\0\\0\\0\end{bmatrix},\begin{bmatrix}0\\1\\0\\0\end{bmatrix},\begin{bmatrix}0\\0\\1\\0\end{bmatrix},\begin{bmatrix}0\\0\\0\\1\end{bmatrix},\begin{bmatrix}-1\\0\\0\\0\end{bmatrix},\begin{bmatrix}0\\-1\\0\\0\end{bmatrix},\begin{bmatrix}0\\0\\-1\\0\end{bmatrix},\begin{bmatrix}0\\0\\0\\-1\end{bmatrix}\right\}.$$

③ The cubature point after iteration of the system equation

$$X^*_{pj,k/k-1} = f\left(X_{pj,k/k-1}, U_k\right) \tag{28}$$

④ The predicted value after time update

$$X^{\wedge}_{p,k/k-1} = \sum_{j=1}^{m} \frac{1}{m} X^*_{pj,k/k-1} \tag{29}$$

⑤ The predicted value of the error covariance matrix

$$P_{p,k/k-1} = \sum_{j=1}^{m} \frac{1}{m} X^*_{pj,k/k-1} X^{*T}_{pj,k/k-1} - X^{\wedge}_{p,k/k-1} X^{\wedge T}_{p,k/k-1} + Q_p \tag{30}$$

where Q_p is the process noise covariance matrix of the road adhesion coefficient.

5) MEASUREMENT UPDATE OF VEHICLE STATE ESTIMATION

Measurements are updated individually in each driving state sub-filter.

① To decompose the predicted covariance matrix based on SVD

$$P_{s,k/k-1} = A_{s,k/k-1} \Lambda_{s,k/k-1} A^T_{s,k/k-1} \tag{31}$$

② The cubature point

$$X_{sj,k/k-1} = A_{si,k/k-1} S_{si,k/k-1} \xi_j + X^{\wedge}_{s,k/k-1} \tag{32}$$

③ The new cubature point based on the measured variables

$$Z_{sj,k/k-1} = h\left(X_{sj,k/k-1}, X^{\wedge}_{sj,k/k-1}, U\,(k)\right) \tag{33}$$

④ The mean of the cubature points

$$Z^{\wedge}_{sj,k/k-1} = \sum_{j=1}^{m} \frac{1}{m} Z_{sj,k/k-1} \tag{34}$$

⑤ The innovation covariance

$$P_{szz,k/k-1} = \sum_{j=1}^{m} \frac{1}{m} Z_{sj,k/k-1} Z^T_{sj,k/k-1} - Z^{\wedge}_{s,k/k-1} Z^{\wedge T}_{s,k/k-1} + R_s \tag{35}$$

where R_s is the measured noise covariance matrix of the driving state.

⑥ The cross-covariance

$$P_{sxz,k/k-1} = \sum_{j=1}^{m} \frac{1}{m} X_{sj,k/k-1} Z^T_{sj,k/k-1} - X^{\wedge}_{s,k/k-1} Z^{\wedge T}_{s,k/k-1} \tag{36}$$

⑦ The filter gain matrix

$$K_{s,k} = P_{sxz,k/k-1} P^{-1}_{szz,k/k-1} \tag{37}$$

⑧ State estimates value after correction of measured variables

$$X^{\wedge}_{s,k} = X^{\wedge}_{s,k/k-1} + K_{s,k}(Z_{s,k} - Z^{\wedge}_{s,k/k-1}) \tag{38}$$

⑨ The error covariance matrix

$$P_{s,k} = P_{s,k/k-1} - K_{s,k} P_{szz,k/k-1} K^T_{s,k} \tag{39}$$

6) MEASUREMENT UPDATE OF ROAD ADHESION COEFFICIENT ESTIMATION

Measurements are updated individually in each road adhesion coefficient sub-filter.

① To decompose the predicted covariance matrix based on SVD

$$P_{p,k/k-1} = A_{p,k/k-1} \Lambda_{p,k/k-1} A^T_{p,k/k-1} \tag{40}$$

② The cubature point

$$X_{pj,k/k-1} = A_{pi,k/k-1} S_{pi,k/k-1} \xi_j + X^{\wedge}_{p,k/k-1} \tag{41}$$

③ The new cubature point based on the measured variables

$$Z_{pj,k/k-1} = h\left(X_{pj,k/k-1}, X^{\wedge}_{pj,k/k-1}, U\,(k)\right) \tag{42}$$

④ The mean of the cubature points

$$Z^{\wedge}_{pj,k/k-1} = \sum_{j=1}^{m} \frac{1}{m} Z_{pj,k/k-1} \tag{43}$$

⑤ The innovation covariance

$$P_{pzz,k/k-1} = \sum_{j=1}^{m} \frac{1}{m} Z_{pj,k/k-1} Z^T_{pj,k/k-1} - Z^{\wedge}_{p,k/k-1} Z^{\wedge T}_{p,k/k-1} + R_p \tag{44}$$

where R_p is the measured noise covariance matrix of the driving state.

⑥ The cross-covariance

$$P_{pxz,k/k-1} = \sum_{j=1}^{m} \frac{1}{m} X_{pj,k/k-1} Z^T_{pj,k/k-1} - X^{\wedge}_{p,k/k-1} Z^{\wedge T}_{p,k/k-1} \tag{45}$$

⑦ The filter gain matrix

$$K_{p,k} = P_{pxz,k/k-1} P^{-1}_{pzz,k/k-1} \tag{46}$$

⑧ State estimates value after correction of measured variables

$$X^{\wedge}_{p,k} = X^{\wedge}_{p,k/k-1} + K_{p,k}(Z_{p,k} - Z^{\wedge}_{p,k/k-1}) \tag{47}$$

⑨ The error covariance matrix

$$P_{p,k} = P_{p,k/k-1} - K_{p,k} P_{pzz,k/k-1} K^T_{p,k} \tag{48}$$

7) INFORMATION FUSION OF VEHICLE STATE ESTIMATION

The local estimated values of each sub-filter in the vehicle driving state are fused through the main filter to obtain the global optimal estimation.

$$P_{sf,k}^{-1} = P_{s1,k}^{-1} + P_{s2,k}^{-1} \tag{49}$$

$$X_{sf,k}^{\wedge} = P_{sf,k}^{-1}\left(P_{s1,k}^{-1}X_{s1,k}^{\wedge} + P_{s2,k}^{-1}X_{s2,k}^{\wedge}\right) \tag{50}$$

8) INFORMATION FUSION OF ROAD ADHESION COEFFICIENT ESTIMATION

The local estimation values of each sub-filter in the road adhesion coefficient are fused through the main filter to obtain the global optimal estimation.

$$P_{pf,k}^{-1} = P_{p1,k}^{-1} + P_{p2,k}^{-1} \tag{51}$$

$$X_{pf,k}^{\wedge} = P_{pf,k}^{-1}\left(P_{p1,k}^{-1}X_{p1,k}^{\wedge} + P_{p2,k}^{-1}X_{p2,k}^{\wedge}\right) \tag{52}$$

Establish the state and measurement equations of the nonlinear system and give the parameters contained in each variable. The formula is shown in (53):

$$\begin{aligned} X_{s/pi,k} &= f\left(X_{s/pi,k-1}, U_{s/pi,k-1}, W_{s/pi,k-1}\right) \\ Z_{s/pi,k} &= h\left(X_{s/pi,k}, v_{s/pi,k}\right) \end{aligned} \tag{53}$$

The state variables of the two sub-filters in the driving state estimator are: $X_{si,k} = [u, v, a_x, a_y, \gamma, \Gamma]$.

The parameter variables of the two sub-filters in the adhesion coefficient estimator are: $X_{p,k} = [\mu_{fl}, \mu_{fr}, \mu_{rl}, \mu_{rr}]$.

The measured variables of sub-filter 1 in the driving state estimator are: $Z_{s,k} = [a_x, a_y, \gamma]$.

The measured variables of sub-filter 2 in the driving state estimator are: $Z_{s,k} = [a_y, \gamma]$.

The measured variables of sub-filter 1 in the adhesion coefficient estimator are: $Z_{p,k} = [a_x, a_y, \dot{\gamma}]$.

The measured variables of sub-filter 2 in the adhesion coefficient estimator are: $Z_{p,k} = [a_y, \dot{\gamma}]$.

The control inputs are: $U_{s/p,k} = [\delta_{fl}, \delta_{fr}, \delta_{rl}, \delta_{rr}, \omega_{fl}, \omega_{fr}, \omega_{rl}, \omega_{rr}]$, where δ_{ij} is the four-wheel angle, which is calculated by the sensor collecting the steering wheel angle signal according to the certain rule.

The determination of the information distribution coefficients is a key issue in the design of the federated filter. A reasonable selection of information distribution coefficients between the main filter and the sub-filters can effectively improve the algorithmic estimation accuracy and fault detection sensitivity of the sub-filters, so as to ensure the optimization of the global estimation. The covariance matrix can reflect the estimation accuracy of each sub-filter to a great extent, so it is used as a measure to calculate the in-formation distribution coefficient. The distribution coefficient in this paper is calculated by using (54).

$$\beta_i = \frac{tr\,(p_i)}{tr\,(p_1) + tr\,(p_2)} \tag{54}$$

where $tr(p_i)$ is the trace of the error covariance matrix and the initial value of the information distribution coefficient is set as: $\beta_1 = \beta_2 = 0$.

IV. SIMULATION VERIFICATION

In order to verify the feasibility and reliability of the proposed estimation algorithm, a corresponding algorithm model was built in the Matlab/Simulink environment. And at the same time, a joint simulation was performed with CarSim to evaluate the effect of the estimation algorithm on the nonlinear driving state of the vehicle. Set the corresponding test conditions and select the dual-line-shifting test conditions of the docking road. The part parameters of the vehicle model are shown in Table 2.

TABLE 2. Part parameters of vehicle model.

Symbol	Parameter Name	Value
m	Vehicle mass (kg)	830
m_s	Sprung mass (kg)	747
L	Front and rear wheelbase (m)	2.34
a	Distance from center of mass to the front axle (m)	1.17
d_1	Front-wheel track (m)	1.416
d_2	Rear-wheel track (m)	1.416
r	Wheel radius (m)	0.278
h	The distance from the center of mass to the ground (m)	0.54
I_z	The rotational inertia of the z-axis (kg/ m2)	1110

For this simulation experimental condition, the parameters are selected as follows: the constant vehicle speed is 30km/h, the road adhesion coefficient is set to 0.5 in the first 110 meters, the last 100 meters is set to 0.3, and the sampling is a fixed step length of 0.01s.

The initial values of two sub-filters in the driving state estimator are selected as:

$$\begin{aligned} X_{s1,0} &= [30/3.6, 0, 0, 0, 0, 0] \\ P_{s1,0} &= eye(6) * 100 \\ Q_{s1,0} &= eye(6) * 100 \\ R_{s1.0} &= diag([0.03, 1, 100]) * 0.01 \end{aligned} \tag{55}$$

$$\begin{aligned} X_{s2,0} &= [30/3.6, 0, 0, 0, 0, 0] \\ P_{s2,0} &= eye(6) \\ Q_{s2,0} &= eye(6) * 100 \\ R_{s2.0} &= diag([1, 70]) * 0.01 \end{aligned} \tag{56}$$

The initial values of two sub-filters in the road adhesion coefficient estimator are selected as:

$$\begin{aligned} X_{p1,0} &= [1, 1, 1, 1] \\ P_{p1,0} &= eye(4) \\ Q_{p1,0} &= eye(4) \\ R_{p1.0} &= diag([0.009, 1, 1]) * 10000 \end{aligned} \tag{57}$$

$$\begin{aligned} X_{p2,0} &= [1, 1, 1, 1] \\ P_{p2,0} &= eye(4) \\ Q_{p2,0} &= eye(4) \\ R_{p2.0} &= eye(2) * 10000 \end{aligned} \tag{58}$$

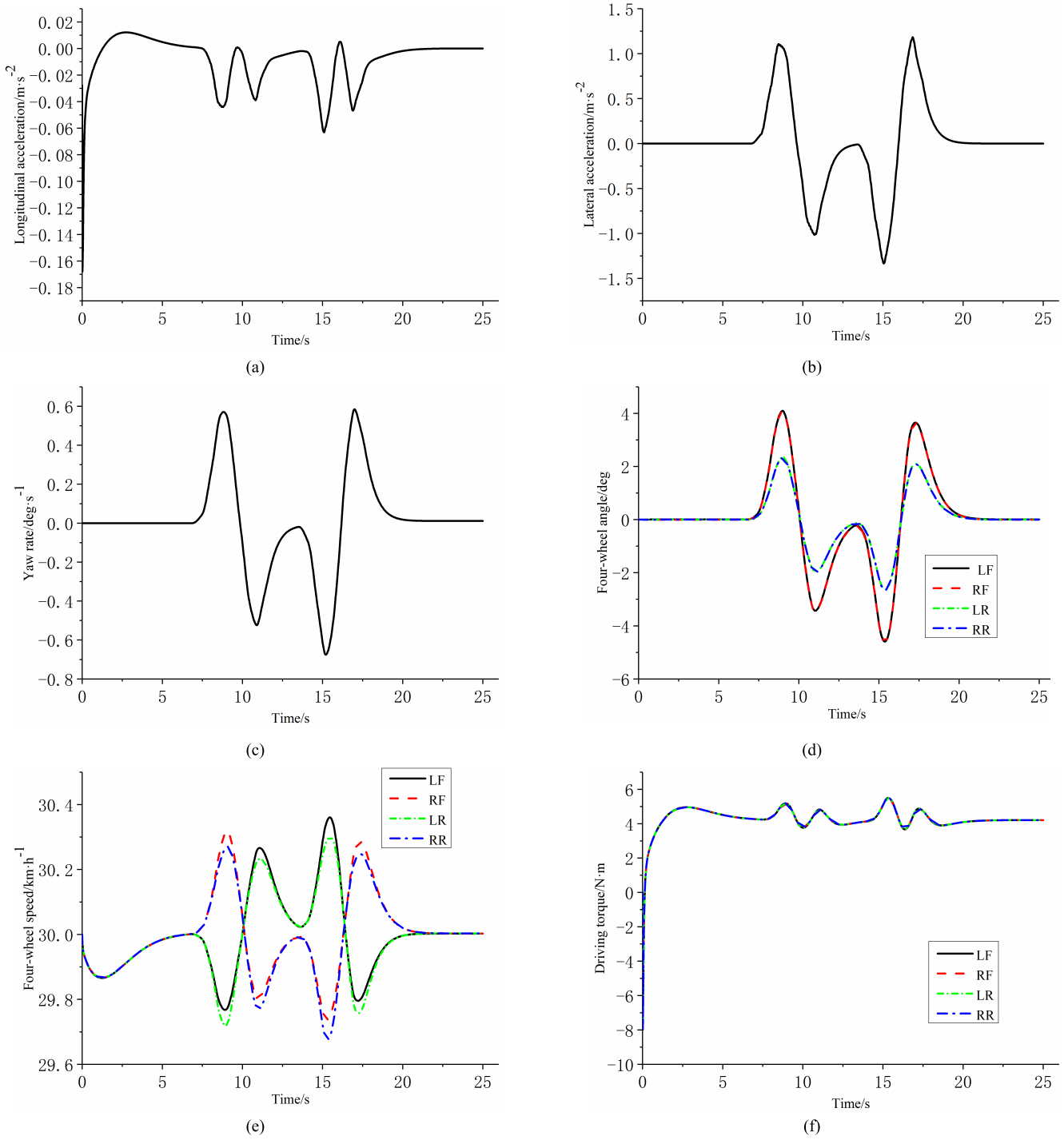

FIGURE 4. Sensor signal: (a) Longitudinal acceleration; (b) Lateral acceleration; (c) Yaw rate; (d) Four-wheel angle; (e) Four-wheel speed; (f) Driving torque.

The simulation experiment results are shown in Fig. 4 and Fig. 5. (a), (b), (c), (d), (e), and (f) in Fig. 5 are the sensor signals output by the CarSim simulation results, that is, the Vehicle-mounted sensor signals collected through the vehicle network. (a), (b), (c), and (d) in Fig. 5 are the comparison results between the estimated values of the vehicle driving state and the road adhesion coefficient obtained by the joint estimation algorithm and the actual value output by CarSim. Fig. 5 (a) is the comparison curve between the estimated value of the longitudinal vehicle speed obtained through the joint algorithm and the actual value output by the vehicle simulation model. From the curve in the figure, it can be seen that the algorithm estimated value has a good effect on stability and accuracy at the initial moment. As the simulated

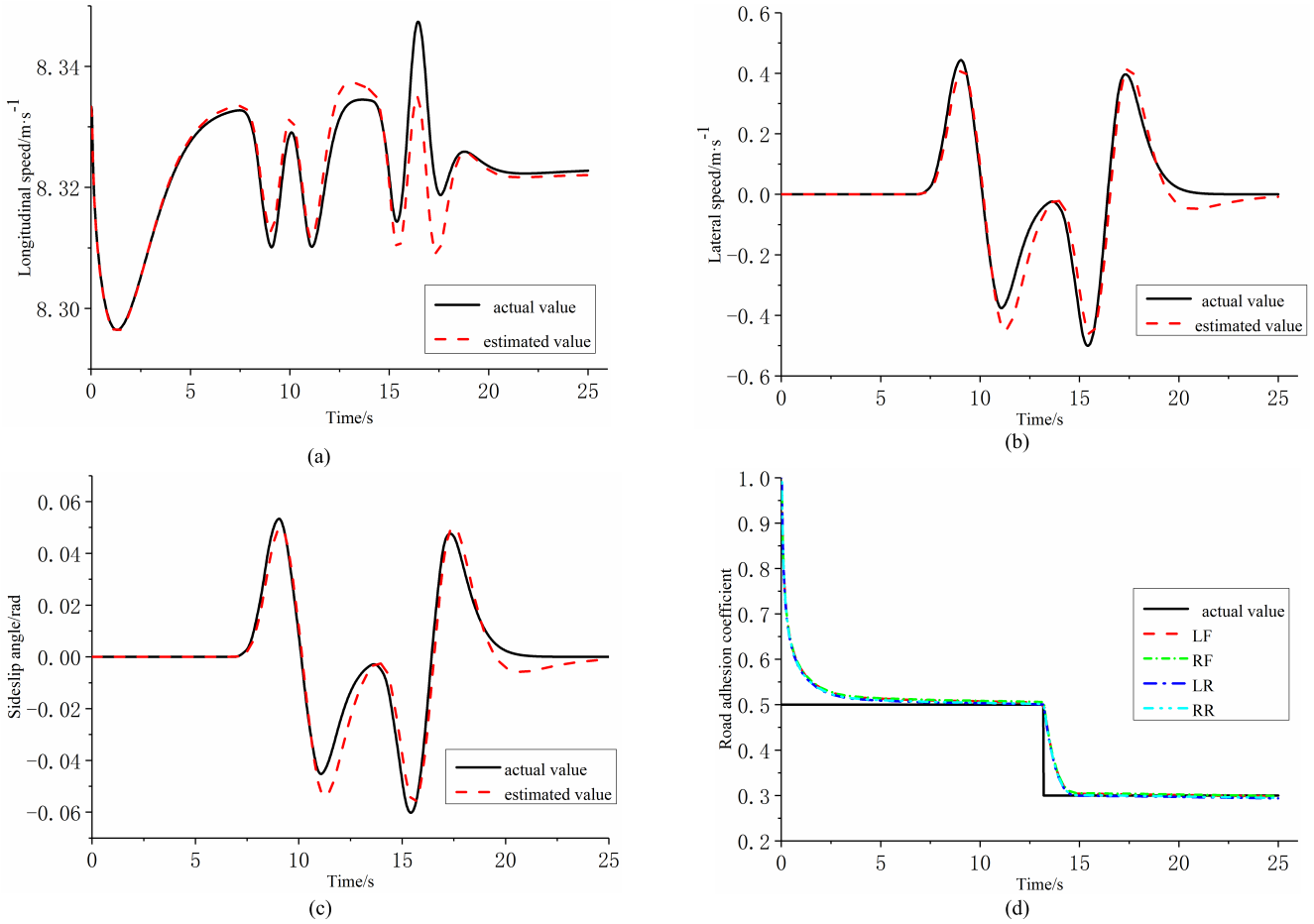

FIGURE 5. Simulation output of vehicle driving state and road adhesion coefficient: (a) Longitudinal speed; (b) Lateral speed; (c) Sideslip angle of centroid; (d) Road adhesion coefficient.

vehicle speed changes become more complex, the estimated value gradually produces a certain error with the true value, but then it returns to a stable state, and the overall effect is good. Fig. 5(b) is the comparison curve between the estimated value of lateral vehicle speed obtained through the joint algorithm and the actual value output by the vehicle simulation model. It can be seen that in addition to a certain delay and error of the estimated value relative to the true value at the peak of the curve, a good estimation effect can be guaranteed at other times. Fig. 5(c) is the comparison curve between the estimated value of the sideslip angle obtained by the joint algorithm and the actual value output by the vehicle simulation model. From the curve in the figure, it can be seen that the estimated value is in good agreement with and the actual value when the vehicle is in a steady state. Only when the curve is at the peak, there is a slight delay and error in the estimated value, but the overall effect of the algorithm estimation is still very good. Fig. 5(d) is the comparison curve between the estimated value of the four-wheel road adhesion coefficient obtained by the joint algorithm and the actual value set by the experimental conditions. It can be seen from the curve in the figure that after the start of the simulation, the estimated values of the four rounds start to track the actual value after about 3s from the initial value and remain stable. After the actual value changes suddenly, its algorithm responds quickly and converges to the actual value in a short time and the error between the two is also very small. The overall estimate effect is good.

V. CONCLUSION

Active safety technology based on vehicle dynamics control has been widely used in automobiles. In order to further reduce control costs and accelerate the maturity of emerging active safety technologies, the paper focuses on the unique dynamics control characteristics of distributed drive electric vehicles and the advantages of multiple information sources, and adopts multi-information fusion technology based on federated Kalman filtering to realize the accurate estimation of the driving state and road adhesion coefficient for the distributed driving electric vehicle.

First, the nonlinear 3-DOF vehicle dynamics model and a Dugoff tire model of distributed drive electric vehicle are established, and the vehicle driving state estimator is designed based on the federated Kalman filter theory. The sub-filter is designed with CKF to improve the accuracy of the algorithm estimation. The vehicle-mounted sensor signals are obtained

through the vehicle network as the input of the estimator, which realizes the accurate estimation of the vehicle driving state.

Second, considering the influence of different roads on the driving state of the vehicle, the road adhesion coefficient estimator is designed based on the federated Kalman filter theory on the basis of the driving state estimation, and the sub-filter adopts CKF. The joint estimation of the two estimators not only improves the adaptability of the estimation algorithm to different roads, but also improves the accuracy and stability of the estimation. In order to further verify the reliability and accuracy of the algorithm, the Matlab/Simulink modular programming software is used to build the joint estimation algorithm model and co-simulate with CarSim for verification under multiple conditions. The results show that the joint estimation algorithm of vehicle driving state and road adhesion coefficient based on federated Kalman filter significantly improves the estimation accuracy and anti-interference of the model, which also proves the effectiveness and accuracy of the algorithm.

Due to the lack of experimental conditions and equipment, the estimation algorithm cannot be verified on the actual vehicle. Future research should mainly establish a dSPACE semi-physical simulation system for distributed drive electric vehicles, and further verify the actual operation effect of the estimation algorithm through hardware-in-the-loop and real vehicle testing. After completing the algorithm test and optimization of the physical hardware system, we will try more vehicle parameters and road condition estimation, and try to apply the algorithm to the big data environment of the Internet of Vehicles.

REFERENCES

[1] Z. P. Yu, Y. Feng, and L. Xiong, "Overview of the development status of distributed drive electric vehicle dynamics control," *J. Mech. Eng.*, vol. 49, no. 8, pp. 105–114, 2013.

[2] P. Q. Hu, Z. F. Tan, G. Qiu, X. Y. Wang, and M. Deng, "Overview of the development of electric vehicles," *Electr. Appl.*, vol. 37, no. 20, pp. 79–85, 2018.

[3] K. B. Singh and S. Taheri, "Estimation of tire–road friction coefficient and its application in chassis control systems," *Syst. Sci. Control Eng.*, vol. 3, no. 1, pp. 39–61, Mar. 2015.

[4] M. Wielitzka, M. Dagen, and T. Ortmaier, "Sensitivity-based road friction estimation in vehicle dynamics using the unscented Kalman filter," in *Proc. Annu. Amer. Control Conf. (ACC)*, vol. 6, Jun. 2018, pp. 2593–2598.

[5] S. Chakraborty, S. Sen, A. Sutradhar, and A. Sengupta, "Estimation of tire-road friction coefficient and frictional force for active vehicle safety system," in *Proc. Int. Conf. Ind. Instrum. Control (ICIC)*, vol. 5, May 2015, pp. 674–679.

[6] G. Li, R. C. Xie, S. Y. Wei, and C. F. Zong, "Estimation of vehicle state and road adhesion coefficient based on dual-cubature Kalman filter," *Technol. Sci.*, vol. 45, no. 4, pp. 403–414, 2015, doi: 10.1360/N092014-00207.

[7] B. L. Gao, H. Chen, S. G. Xie, and J. F. Gong, "Fusion estimation of distributed electric drive vehicle speed and road adhesion coefficient," *Automot. Eng.*, vol. 38, no. 2, pp. 216–220, 2016, doi: 10.3969/j.issn.1000-680X.2016.02.014.

[8] X. Fu, W. Sun, B. Huang, A. J. Xing, and J. Wang, "Estimation of road adhesion coefficient based on exponentially weighted decay memory unscented Kalman filter," *Automobile Technol.*, no. 1, pp. 31–37, 2018, doi: 10.19620/j.cnki.1000-3703.20170512.

[9] X. Y. Ping, L. Li, S. Chen, and H. Y. Wang, "Research on road adhesion coefficient identification of four-wheel Independent drive vehicles in multiple working conditions," *J. Mech. Eng.*, vol. 55, no. 22, pp. 80–92, 2019.

[10] F. Lin and C. Huang, "Use UKF algorithm to estimate road adhesion coefficient," *J. Harbin Inst. Technol.*, vol. 45, no. 7, pp. 115–120, 2013.

[11] L. Yao, "Research on the state estimation method of four-wheel in-wheel motor electric vehicle," M.S. thesis, Jilin Univ., Changchun, China, 2015.

[12] X. J. Yang, J. Y. Li, K. Zhang, and T. Liao, "Research on vehicle adaptive cruise control based on estimation of road adhesion coefficient," *J. Nanjing Univ. Sci. Technol.*, vol. 42, no. 4, pp. 466–473, 2018, doi: 10.14177/j.cnki.32-1397n.2018.42.04.012.

[13] W. W. Chen, X. Y. Liu, H. Huang, and J. Yang, "Estimation algorithm of road adhesion coefficient under vehicle turning conditions," *Automot. Eng.*, vol. 33, no. 6, pp. 521–526, 2011.

[14] B. Li, H. Du, and W. Li, "A novel cost effective method for vehicle tire-road friction coefficient estimation," in *Proc. IEEE/ASME Int. Conf. Adv. Intell. Mechatronics*, Jul. 2013, pp. 1528–1533.

[15] F. Wang, "Research on vehicle integrated navigation algorithm based on federated Kalman filter," M.S. thesis, Harbin Eng. Univ., Harbin, China, 2019.

[16] Z. G. Ao, C. C. Tang, C. Q. Fu, J. Guo, and C. L. Ye, "Multi-sensor adaptive cubature Kalman filter fusion algorithnm," *Appl. Res. Comput.*, vol. 31, no. 5, pp. 1312–1315, 1331, 2016.

[17] Z. S. Yu, *Automobile Theory*. Beijing, China: Machinery Industry Corporation, 2009, pp. 144–146.

[18] W. B. Chu, "State estimation and coordinated control for distributed electric vehicles," M.S. thesis, Tsinghua Univ., Beijing, China, 2013.

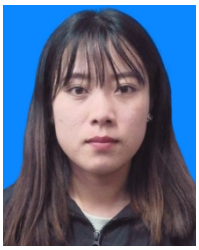

YANAN WU is currently pursuing the degree with the Liaoning University of Technology.

GANG LI received the M.S. degree in vehicle engineering from the Liaoning University of Technology, Jinzhou, China, in 2006, and the Ph.D. degree in vehicle engineering from Jilin University, Changchun, China, in 2013. He is currently a Professor and the Dean of the College of Automobile and Traffic Engineering, Liaoning University of Technology. He has authored or coauthored more than 50 journal articles and conference papers. He was a recipient of 30 China patents and software copyrights. He is in charge of numerous projects funded by national government and institutional organizations on electric vehicles and energy management systems. His current research interests include model, simulation, intelligent control for vehicles, and vehicle active safety.

DONGSHENG FAN received the M.S. degree in vehicle engineering from the Liaoning University of Technology, Jinzhou, China, in 2020. He is currently working in Beijing.